Available online at www.sciencedirect.com
SCIENCE DIRECT®
International Journal of Mass Spectrometry 228 (2003) 35–47
International Journal of Mass Spectrometry
www.elsevier.com/locate/ijms

On gaseous $C_4H_6O_2$ compounds in the atmosphere: new insights from collision experiments of the protonated molecules in the laboratory and on aircraft

Detlef Schröder[a,*], Héloïse Soldi-Lose[a], Marija Semialjac[a], Jessica Loos[a], Helmut Schwarz[a], Gunter Eerdekens[b], Frank Arnold[b,1]

[a] *Institut für Chemie der Technischen Universität Berlin, 10623 Berlin, Germany*
[b] *Max-Planck-Institut für Kernphysik, Abt. Atmosphärenphysik, 69129 Heidelberg, Germany*

Received 27 February 2003; accepted 25 March 2003

Dedicated to F. W. McLafferty on the occasion of his 80th birthday.

Abstract

A variety of mass spectrometric methods and complementary theoretical calculations are used to assess the potential contributions of $C_4H_6O_2$ isomers to the $m/z = 87$ ion found in a recent atmospheric field study (Int. J. Mass Spectrom. 223/224 (2003) 733). The analysis of high- and low-energy collision experiments suggests that a ca. 1:1:1 mixture of crotonic acid, vinylacetic acid, and methyl acrylate can account for the experimental findings in the field study. For a more concise assessment, further field studies using complementary approaches for the characterization of atmospheric trace components are recommended.

Keywords: $C_4H_6O_2$; Atmospheric chemistry; Carboxylic acids; Chemical ionization; Collision-induced dissociation; Density functional theory

1. Introduction

Oxygenated volatile organic compounds (OVOCs) present in the terrestrial atmosphere are potentially important as they may influence ozone and aerosols and thereby also climate. One example is acetone which has been detected in the free troposphere and the lower stratosphere by means of chemical-ionization mass spectrometry (CI-MS) [1–3]. In the upper troposphere, acetone represents a major, if not the most dominant source of $HO_2^\bullet$ and $OH^\bullet$ radicals. The latter influences both the formation and loss of ozone as well as the formation of gaseous sulfuric acid which in turn influences aerosol formation and growth. However, for OVOCs containing three or more carbon atoms, the mere measurement of mass-to-charge ratios (m/z) of the protonated molecules by means of CI-MS is insufficient for an unambiguous identification. Accordingly, it is a crucial demand to develop methods which cannot only detect but also structurally identify volatile organic compounds present in the atmosphere as very minor impurities.

* Corresponding author. Tel.: +49-30-314-26546; fax: +49-314-21102.
E-mail address: df@www.chem.tu-berlin.de (D. Schröder).
[1] Co-corresponding author.

1387-3806/03/$ – see front matter © 2003 Elsevier Science B.V. All rights reserved.
doi:10.1016/S1387-3806(03)00192-1

Additional insight into molecular structures can be achieved by MS/MS studies, particularly collision-induced dissociation (CID) of mass-selected ions [4,5]. In order to exploit the usefulness of CID for atmospheric OVOC measurements, a novel aircraft-borne CI-MS instrument based on an ion trap (IT) mass spectrometer has been designed by the Max-Planck-Institut für Kernphysik. In this device, an analyte X is detected indirectly as the protonated species $[X + H]^+$ formed in the reaction with H_3O^+. During the first test flights [6], the instrument allowed the detection of several OVOCs. These included acetone (A) with $m/z = 59$ for the protonated molecule and a trace gas X with $m/z = 87$ for the protonated form. While the identity of compound X is unknown, CID studies were made for $[A + H]^+$ and $[X + H]^+$ in flight. It is important to note that throughout this contribution the observed $[X + H]^+$ signal is assumed to be formed by protonation of one or several neutral compounds X with a mass of 86 amu according to reaction (1). However, we cannot exclude the occurrence of dissociative protonation in CI-MS. Specifically, Spanel and Smith [7,8] have demonstrated that gas-phase protonation of alkanols, carboxylic acids, etc. can also lead to direct dehydrations. Consequently, instead of neutral X with 86 amu, protonation of a neutral compound Y with a mass of 104 amu (reaction 2) may lead to the fragment $[Y + H - H_2O]^+$, again with $m/z = 87$.[2]

$$H_3O^+ + X \rightarrow [X + H]^+ + H_2O \quad (1)$$

$$H_3O^+ + Y \rightarrow [Y + H - H_2O]^+ + 2H_2O \quad (2)$$

The present paper specifically deals with some attempts towards an identification of the protonated molecule $[X + H]^+$ with $m/z = 87$. To this end, the atmospheric data are complemented by laboratory CID experiments and ab initio studies.

[2] Likewise, esters can undergo loss of the corresponding alkanols upon dissociative protonation [8], which would mean that $[Y' + H - ROH]^+$ is sampled.

2. Experimental and theoretical methods

The aircraft-borne mass spectrometer is an ion trap instrument which relies on the principles of proton-transfer mass spectrometry (PT-MS [9,10]). Initially, water vapor is ionized by bombardment with electrons followed by rapid ion/molecule reactions leading to an abundant signal for H_3O^+ ($m/z = 19$) along with some clustering to $(H_2O)H_3O^+$ ($m/z = 37$). Then, H_3O^+ serves as a primary ion which is able to protonate all molecules X whose proton affinities PA(X) exceed $PA(H_2O) = 165.2$ kcal/mol [11]. MS/MS experiments were performed by mass selection of the ions of interest followed by an excitation sweep, allowance of sufficient time for energizing collisions, and ion detection. In the CID experiments, helium was present as collision gas in the ion trap at a pressure of ca. 2×10^{-5} mbar.

In the laboratory studies, initial experiments were performed with a modified VG ZAB/HF/AMD 604 four-sector mass spectrometer of BEBE configuration (B stands for magnetic and E for electric sector) described previously [12]. In brief, ca. 1 mg of the neutral $C_4H_6O_2$ isomers was introduced together with ca. 50 μl water via a septum inlet system to a chemical ionization (CI) source in which the neutrals were ionized by electrons having a kinetic energy of 100 eV at a repeller voltage of ca. 0 V. After acceleration to 8 keV kinetic energy, the $m/z = 87$ ions were mass selected using B(1) and E(1) and characterized by collisional activation (CA). To this end, the fast-moving cations were collided with helium at 80% transmittance and the fragments were monitored by scanning B(2). The spectra were recorded and on-line processed with the AMD/Intectra data system; 8–20 scans were accumulated. Though metastable ion spectra were recorded also, their contributions to the CA experiments do not alter the qualitative isomer distinctions made further below and are therefore omitted.

Collision-induced dissociation (CID) at low collision energies was performed using a VG BIO-Q mass spectrometer [13], which consists of an electrospray ionization (ESI) source combined with a tandem mass spectrometer of QHQ configuration (Q stands for

quadrupole and H for hexapole). In the present experiments, millimolar solutions of $C_4H_6O_2$ neutrals in pure water were introduced through a stainless steel capillary to the ESI source via a syringe pump (ca. 5 μl/min). Nitrogen was used as nebulizer and as drying gas at source temperatures of 80–100 °C. Optimal yields of the desired $C_4H_7O_2^+$ species were achieved by adjusting the cone voltage to about 30 V. At lower cone voltages, proton-bound dimers prevail, e.g., $C_4H_7O_2^+ \cdot H_2O$ ($m/z = 105$) and $C_4H_7O_2^+ \cdot C_4H_6O_2$ ($m/z = 173$), whereas excessive dissociation occurs at higher cone voltages. For CID, $C_4H_7O_2^+$ was mass selected using Q1, interacted with argon as a collision gas in the hexapole under single-collision conditions (typically 4×10^{-4} mbar) at variable collision energies ($E_{lab} = 0$–50 eV), while scanning Q2 to monitor the ionic products.

For reasons becoming obvious further below, complementary ab initio calculations were performed with the B3LYP hybrid functional which relies on Becke's three parameter fit and the correlation part due to Lee et al. and Becke [14,15] as implemented in the GAUSSIAN 98 suite of programs [16]. Full geometry optimizations and frequency calculations were performed using triple-ζ basis sets with diffuse functions included (6-311++G**). Thus, the relative energies of the stationary points listed below correspond to the B3LYP/6-311++G** level of theory with inclusion of zero-point energy (ZPE) at 0 and 298 K. Note, however, that we have not explored the entire conformational space and instead restricted ourselves to the presumably most stable *all-anti* conformations.

3. Aircraft-based atmospheric measurements

In the field studies, both ions $[A+H]^+$ and $[X+H]^+$ were found to decrease steeply in concentration above the tropopause [6]. Accordingly, the corresponding trace gases A and X have tropospheric sources and stratospheric sinks. The latter leads to a molecular lifetime which is shorter than the vertical exchange timescale due to convection. In the case of acetone, this sink is mostly due to photolysis along with some attack by nascent hydroxyl radicals which lead to a photochemical lifetime of 15–20 days for acetone in 10 km altitude. We note in passing that the tropopause behavior strongly suggests A and X as real atmospheric gases, rather than being due to contaminations or instrumental artifacts.

The CID spectrum of the $[X+H]^+$ ion with $m/z = 87$ recorded during the flight at an altitude of about 10 km shows fragment ions at $m/z = 69$, 55, 45, and 43 corresponding to mass differences of $\Delta m = 18$, 32, 42, and 44, respectively (Fig. 1; [6]). In the following, we refer to these fragments as those of the "atmospheric ion."

Some information about the elemental composition of $[X + H]^+$ can be derived from an analysis of the isotope envelopes of the ion signal. For the $m/z = 87$ ion, the measured abundance ratio of $^{13}C_1$-isotopolog at $m/z = 88$ corresponds to $A_{88}/A_{87} = 3.8 \pm 0.2\%$ indicating the presence of three to four carbon atoms in the corresponding neutral molecule X. Thus, while protonated acetone is known to be formed in CI-MS of atmospheric gases, the ^{13}C pattern of the $m/z = 87$ ion disfavors an assignment of the homologous ketone. If, for example, $[X+H]^+$ were protonated pentanone, natural isotope abundances would imply a relative abundance of 5.6% of the neighboring ^{13}C peak at $m/z = 88$ [17], compared to only $3.8 \pm 0.2\%$ observed for the atmospheric ion. Further, the isotope patterns do not provide any indications for the participation of heavier elements, e.g., sulfur or chlorine, and the fragmentation scheme gives no hint towards the presence of fluorine (e.g., loss of HF, $\Delta m = 20$). Hence, we confine ourselves to CHNO compounds. With the assumption that the ionization conditions in the air-borne mass spectrometer only afford protonation of long-lived neutral molecules present in the atmosphere, thereby leading to closed-shell ions, the ion mass excludes the presence of an odd number of nitrogen atoms.

Assuming the presence of carbon, hydrogen, oxygen, and an even number of nitrogen atoms, conceivable formulae for $m/z = 87$ are $C_2H_3N_2O_2^+$, e.g., protonated nitroacetonitrile $[\mathbf{1} + H]^+$ (Scheme 1), $C_3H_7N_2O^+$, e.g., protonated α-aminopropiolactam

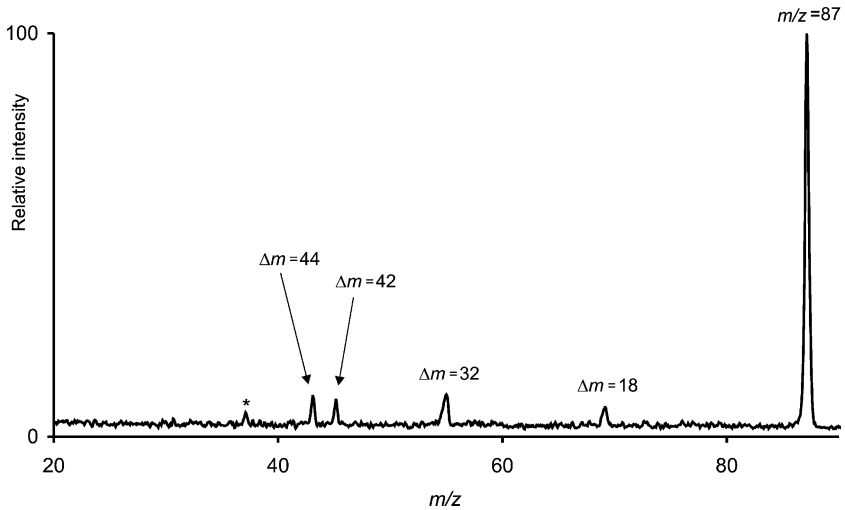

Fig. 1. CID spectrum of the $m/z = 87$ ion formed by proton-transfer from incident H_3O^+ with trace components in the atmosphere sampled at an altitude of approximately 10 km in an air-borne IT-MS. Note that the collision energy in the actual experiment is not well-defined because it was necessary to operate in the multicollision regime in order to achieve the maximal sensitivity. The signal at $m/z = 37$ (designated by an asterisk) is attributed to collision-induced proton transfer from the $C_4H_7O_2^+$ ions to water followed by rapid clustering of H_3O^+ to afford the proton-bound dimer $(H_2O)H_3O^+$ (see text).

$[\mathbf{2} + H]^+$, $C_4H_{11}N_2^+$, e.g., protonated butyramidine $[\mathbf{3} + H]^+$, $C_3H_3O_3^+$, e.g., protonated malonic anhydride $[\mathbf{4} + H]^+$, and $C_4H_7O_2^+$ isomers. For the following reasons, we restrict ourselves to the latter formula. (i) The composition $C_2H_3N_2O_2^+$ cannot cope with the $^{13}C/^{12}C$ ratio of the $m/z = 87$ ion. (ii) For the hydrogen-rich ions, $C_3H_7N_2O^+$ and $C_4H_{11}N_2^+$, one would expect losses of ammonia ($\Delta m = 17$) or other neutral fragments of odd masses which are not observed in Fig. 1. While we do not rigorously exclude $C_3H_3O_3^+$, the composition $C_4H_7O_2^+$ for the $m/z = 87$ ion appears much more plausible, because loss of H_2O seems unlikely for the former. Therefore, the following analysis is limited to $C_4H_7O_2^+$ ions. Notwithstanding, some of the above mentioned formulae could explain the deviation of the experimentally found $^{13}C/^{12}C$ ratio ($3.8 \pm 0.2\%$) from the value of 4.5% expected, if the $m/z = 87$ ion were entirely due to $C_4H_7O_2^+$ isomers [17].

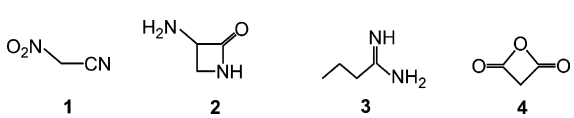

Scheme 1.

4. Laboratory studies

Although the net formula $C_4H_7O_2^+$ might not appear too complex, quite a significant number of isomers is conceivable of which we have not covered all. Because the investigation evolved in several stages using different methods, let us follow this development in order to substantiate the selection of isomers made.

4.1. High-energy CA

For a rapid screening of the fragmentation patterns of $C_4H_7O_2^+$ ions as a first stage, these ions were generated by protonation of the neutral $C_4H_6O_2$ precursors **5**–**16** (Scheme 2) using H_2O as reagent gas in the CI source of a sector field mass-spectrometer. CA of the mass-selected $C_4H_7O_2^+$ ions at high kinetic energies (8 keV) was then used to probe dissociation behaviors and hence differentiate ion structures. We note

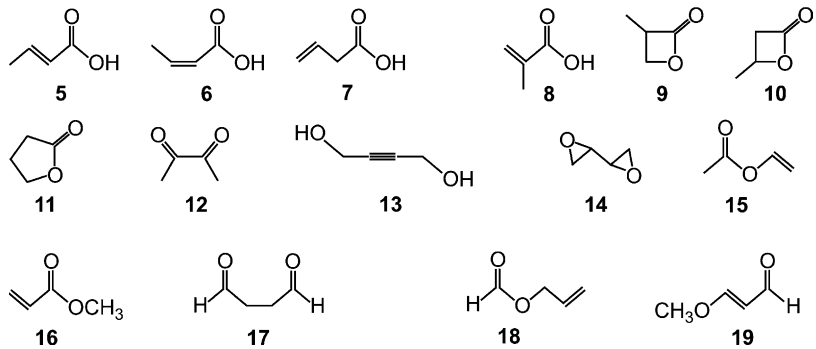

Scheme 2.

in passing that the CA patterns of some $C_4H_7O_2^+$ ions have previously been examined in a different context [18–20].

The use of a sector instrument in the first stage has several advantages: (i) decreased probability of termolecular reactions occurring upon or shortly after ionization due to the relatively low operating pressures in conventional CI sources, (ii) preference of direct bond cleavages over extensive rearrangements in high-energy collision experiments, (iii) the ability to gain additional information rather than just mere mass differences from peak-shape analysis, and (iv) limited memory effects in the inlet system. Particularly, the latter aspect is all but trivial for polar compounds such as most $C_4H_6O_2$ isomers, in that the removal of the samples from the inlet systems may require considerable amounts of time. In sector-field MS, several minutes of pumping and subsequent purging with the next sample is sufficient for this purpose.

The CA patterns of the $C_4H_7O_2^+$ ions generated from the precursors **5**–**16** allow for a qualitative classification (Table 1). To this end, the observed mass differences are assigned as follows: $\Delta m = 18$ is attributed to loss of H_2O, $\Delta m = 28$ can be due to the expulsion of C_2H_4 and/or CO, $\Delta m = 30$ corresponds to the loss of CH_2O, $\Delta m = 32$ to elimination of CH_3OH or, less likely, O_2, $\Delta m = 42$ can be explained by the formation of neutral C_3H_6 and/or CH_2CO, and finally, $\Delta m = 44$ is attributed to losses of C_2H_4O and/or CO_2. In addition, $\Delta m = 46$ is listed which can be regarded as a measure for the consecutive fragmentations of $C_3H_7^+$ ($\Delta m = 44$) by elimination of H_2 and of $C_4H_5O^+$ ($\Delta m = 18$) by loss of CO to yield the allyl cation $C_3H_5^+$ ($\Delta m = 46$) in both cases [18–20].

The spectra of the *E*- and *Z*-isomers of protonated crotonic acid $[\mathbf{5} + H]^+$ and $[\mathbf{6} + H]^+$ are dominated by losses of water to afford a conjugated acyl cation (Scheme 3a). Additional signals due to $\Delta m = 42$ and 44 are assigned to losses of C_3H_6 and CO_2, respectively, where the assignment of the neutral fragments

Table 1
Structure-indicative fragments[a] (given as mass differences Δm) in the high-energy CA mass spectra (8 keV, sector-field instrument) of mass-selected $C_4H_7O_2^+$ ions generated by CI of the neutral compounds **5**–**16** using water as reagent gas

	18	28	30	32	42	44	46
$[\mathbf{5} + H]^+$	100	1	1	2	30	35	15
$[\mathbf{6} + H]^+$	100	1	1	3	25	35	15
$[\mathbf{7} + H]^+$	50	3	1	1	30	100	8
$[\mathbf{8} + H]^+$	100	50[b]	1	7	45	40	30
$[\mathbf{9} + H]^+$	80	100	2	8	55	90	40
$[\mathbf{10} + H]^+$	30	5[b]		2	15	100	2
$[\mathbf{11} + H]^+$	25	5[c]	1	8	45	100	8
$[\mathbf{12} + H]^+$	35	75		3	20	100	8
$[\mathbf{13} + H]^+$[d]	100	10[b]	1	4	55	95	25
$[\mathbf{14} + H]^+$	45	5[c]	40	7	45	100	20
$[\mathbf{15} + H]^+$[e]	2			1	3	100	1
$[\mathbf{16} + H]^+$	2	5[c]		100	5	2	1

[a] Normalized to the base peak (=100).
[b] Dished-top peak due to a large KER.
[c] Broadened peak due to a notable KER.
[d] In addition, 4% of $\Delta m = 36$ (loss of two H_2O molecules) is observed as a structure-indicative signal of this ion.
[e] In addition, 2% of $\Delta m = 26$ (loss of C_2H_2) is observed as a structure-indicative signal of this ion.

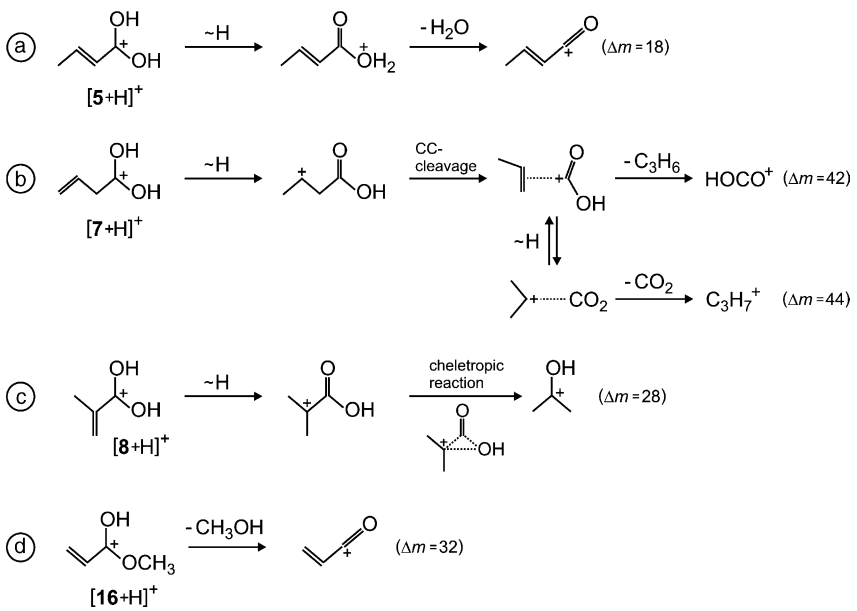

Scheme 3.

is based on the behavior of related crotylamide ions [21]. While protonated vinylacetic acid $[\mathbf{7} + \mathrm{H}]^+$ leads to a similar pattern, the C_3H_6 and CO_2 losses are much more pronounced for this ion. These products can be attributed to an intramolecular proton transfer from the carbonyl group to the terminal double bond leading to a carbenium ion intermediate which can then decompose via ion-neutral complexes (Scheme 3b) [22]. For protonated methacrylic acid $[\mathbf{8} + \mathrm{H}]^+$, a pronounced loss of carbon monoxide is observed which is ascribed to hydrogen migration followed by a cheletropic reaction to presumably generate protonated acetone (Scheme 3c). The loss of CO from $[\mathbf{8} + \mathrm{H}]^+$ is associated with a characteristic peak broadening of the $\Delta m = 28$ signal due to a substantial kinetic energy release (KER) which is specific for this particular ion [18–20]. In summary, the $C_4H_6O_2$ acids studied here can clearly be distinguished from each other, except for the differentiation between the *E*- and *Z*-isomers of crotonic acid which is beyond interest in the present context.

The CA spectra of the corresponding protonated lactones $[\mathbf{9} + \mathrm{H}]^+$–$[\mathbf{11} + \mathrm{H}]^+$ bear fragmentation patterns similar to those of $[\mathbf{5} + \mathrm{H}]^+$–$[\mathbf{8} + \mathrm{H}]^+$, suggesting proton-mediated ring-openings of the cyclic isomers. Protonated β-butyrolactone $[\mathbf{10} + \mathrm{H}]^+$, for example, shows losses of H_2O, C_3H_6, and CO_2 which can be attributed to the protonated butenoic acids $[\mathbf{5} + \mathrm{H}]^+$–$[\mathbf{7} + \mathrm{H}]^+$, but also leads to the expulsion of CO characteristic for $[\mathbf{8} + \mathrm{H}]^+$.

Other conceivable $C_4H_6O_2$ isomers arise from two topological approaches. Maintaining the C_4-skeleton, viz. dislocation of the oxygen atoms, inter alia leads to diacetyl **12**, the butynediol **13**, and the diepoxybutane **14**. Cleavage of the C_4-skeleton by oxygen insertion can, for example, give rise to vinyl acetate **15** and methyl acrylate **16**. All these isomers display characteristic CA patterns. Thus, the CA spectrum of protonated diacetyl, $[\mathbf{12} + \mathrm{H}]^+$, is dominated by losses of acetaldehyde ($\Delta m = 44$) and CO ($\Delta m = 28$) where the latter can clearly be distinguished from the corresponding fragmentation of $[\mathbf{8} + \mathrm{H}]^+$ because the peak broadening is considerably smaller for the CO loss from $[\mathbf{12} + \mathrm{H}]^+$ in comparison to $[\mathbf{8} + \mathrm{H}]^+$. Not surprisingly, fragmentation of the protonated diol $[\mathbf{13} + \mathrm{H}]^+$ is governed by loss of water, and the protonated

bisepoxide $[\mathbf{14}+\mathrm{H}]^+$ can be identified by a characteristic expulsion of formaldehyde ($\Delta m = 30$). Protonated vinyl acetate $[\mathbf{15}+\mathrm{H}]^+$ almost exclusively gives rise to $\Delta m = 44$ which is attributed to the formation of acetyl cation concomitant with loss of neutral C_2H_4O, presumably acetaldehyde or its enol. Finally, the fragmentation behavior of $[\mathbf{16}+\mathrm{H}]^+$ is unique in that an intense loss of neutral methanol ($\Delta m = 32$) occurs for this particular ion (Scheme 3d).

In summary, most of the $C_4H_7O_2^+$ isomers can qualitatively be distinguished by means of their CA spectra. Of course, many other ion structures are conceivable and several of these might also be experimentally accessible. Nevertheless, we pragmatically restrict ourselves to $[\mathbf{5}+\mathrm{H}]^+$–$[\mathbf{16}+\mathrm{H}]^+$ because already this set of isomers is sufficient to account for the CID pattern of the atmospheric ion with $m/z = 87$ (Fig. 1).

4.2. Plausibility considerations

The atmospheric field studies suggest that the $m/z = 87$ ion arises from one or several neutral $C_4H_6O_2$ molecules present as trace components in the earth's atmosphere up to 10 km altitude [6]. Consequently, these molecules need to be reasonably stable with respect to oxidative, hydrolytic, as well as photolytic degradations and must further bear realistic heats of formation (ΔH_f) engendering their presence in the atmosphere. As a second stage, some plausibility considerations based on chemical and thermodynamic criteria are used for a pre-selection of the most likely candidates. Succinic dialdehyde **17**, for example, not only is anticipated to be considerably less stable than diacetyl (**12**), but considered unlikely to persist in significant concentrations in the oxidizing atmosphere of earth. Similarly, we neglect the participation of other aldehydes as well as formates (e.g., **18**). Likewise, enol ethers such as 3-methoxyacrolein **19** are expected to undergo rapid hydrolysis in the atmosphere. Compounds such as the butynediol **13** or the bisepoxide **14**, on the other hand, have unfavorable heats of formation, and it simply does not appear plausible that they occur in significant concentrations.

However, the heats of formation (ΔH_f) of gaseous $C_4H_6O_2$ neutrals listed in literature compilations [23,24] do not cover all isomers considered here and several values are based on thermochemical extrapolation schemes. More troublesome is that some data appears to oppose chemical intuition. For example, the Lias compendium [23] lists identical heats of formation for *E*-crotonic acid **5** and vinylacetic acid **7**, although the former bears a conjugated π-system with an internal double bond, while the latter lacks conjugation and has a terminal vinyl group, both considered to cause destabilization of **7** relative to **5**. In order to settle the situation somewhat more definitively, the neutral compounds **5**–**19** were, therefore, studied computationally at the B3LYP/6-311++G** level of theory which is expected to yield chemically accurate (±2 kcal/mol) relative energies for simple organic compounds [25–27], particularly for the closed-shell $C_4H_6O_2$ molecules of interest here [28].

Upon comparison of the relative energies compiled in Table 2, most of the data agrees pretty well with experiment as expected for the B3LYP approach. It is also obvious, however, that some of the experimental data is doubtful. For example, B3LYP predicts **5** to be about 10 kcal/mol more stable than **7** which precisely follows chemical intuition of the differential stabilization of these acids, whereas the thermochemical compilations suggest $\Delta H_f(\mathbf{5}) \approx \Delta H_f(\mathbf{7})$. In order to allow for a more direct comparison, we deliberately anchor the computed energetics to the apparently most accurate literature values, i.e., those of **5**, **8**, **12**, and **15** in ref. [24]. As expected, "chemical accuracy" is achieved with this scheme in that most experimental and computed ΔH_f values agree nicely. Notable exceptions are vinylacetic acid **7** and methyl acrylate **16**, which theory predicts to be considerably less stable than inferred from experiment. Given the generally good performance of theory in this respect, re-consideration of the experimental figures appears indicated.

With respect to the present context, the computations reveal that highly unsaturated or strained isomers, e.g., **13** and **14**, are unlikely to appear in the earth's atmosphere based on thermochemical

Table 2
Relative energies (E_{rel} in kcal/mol at 0 and 298 K, respectively)[a] of the neutral $C_4H_6O_2$ isomers[b] calculated at the B3LYP/6-311++G** level of theory, computationally predicted heats of formation ($\Delta H_{f,298}^{theory}$ in kcal/mol)[c], experimental values given in the literature ($\Delta H_{f,298}^{expt}$ in kcal/mol),[d] and the difference between theory and experiment ($\Delta\Delta H^{theory/expt}$ in kcal/mol).

	$E_{rel,0\,K}$	$E_{rel,298\,K}$	$\Delta H_{f,298}^{theory}$	$\Delta H_{f,298}^{expt}$	$\Delta\Delta H^{theory/expt}$
5[e]	0.0[f]	0.0	−87.3	−88.1	0.8
6[g]	2.1	1.9	−85.2	−87[h]	1.9
7	10.1	10.0	−77.2	−84[i]	6.9
8[j]	2.1	2.0	−85.2	−87.8	2.6
9	11.5	10.9	−75.8		
10	14.8	14.4	−72.5		
11	2.2	1.3	−85.1	−87.0	1.9
12	7.1	7.6	−80.2	−78.1	−2.1
13	59.2	60.1	−28.1		
14	68.4	67.8	−18.9		
15	10.8	11.0	−76.5	−75.3[i]	−1.2
16[k]	13.6	13.7	−73.7	−79.6	5.9
17	16.3	16.5	−71.0		
18	20.0	20.0	−67.3		
19	29.9	30.0	−57.4		

[a] Including ZPE.
[b] Based on chemical intuition and experience [28], we attempted to select the most stable *all-anti* conformers. However, we have not excessively explored the conformational space and cannot exclude the existence of more stable conformers in a strict sense.
[c] Computational predictions anchored to the values of isomers **5**, **8**, **12**, and **15** as the apparently most accurate ones.
[d] Ref. [24].
[e] *All-anti*-conformer; a second conformer with a 180°-rotated carboxy group is 0.4 kcal/mol higher in energy.
[f] Total energy: −306.5856247 Hartree.
[g] A second conformer with a 180°-rotated carboxy group is 1.1 kcal/mol higher in energy.
[h] Value relative to **5**, using the $\Delta H_{f,298}^{expt}$ difference between **5** and **6** given in ref. [23].
[i] Ref. [23].
[j] OH-group oriented towards the methylene group; a second conformer with 180°-rotated carboxy group is 0.5 kcal/mol higher in energy.
[k] *All-anti*-conformer; a second conformer with 180°-rotated carboxymethyl group is 0.7 kcal/mol higher in energy.

considerations. Pragmatically considering ≥20 kcal/mol above the most stable isomer **5** as a cutoff criterion, we thus remain with isomers **5**–**12** and **15**–**17**. Next, we exclude the aldehyde **17** because it is not expected to be long-lived in the atmosphere. Likewise, the lactones **9**–**11** as well as the enol ester **15** are neglected since rapid hydrolysis is assumed to occur in the atmosphere. Finally, consideration of the difference of *E*- and *Z*-crotonic acid is beyond the scope of this study. Hence, we remain with the acids **5**, **7**, and **8** as well as diacetyl **12** and methyl acrylate **16**; the latter is obviously required to account for the $\Delta m = 32$ signal observed in Fig. 1.

For these five compounds, we also computed the relative stabilities of their protonated forms using the B3LYP approach: $E_{rel}([\mathbf{5} + H]^+) = 0.0$ kcal/mol ($E_{tot} = -306.9093178$ H), $E_{rel}([\mathbf{7} + H]^+) = 9.5$ kcal/mol, $E_{rel}([\mathbf{8} + H]^+) = 6.4$ kcal/mol, $E_{rel}([\mathbf{12} + H]^+) = 15.8$ kcal/mol, $E_{rel}([\mathbf{16} + H]^+) = 15.0$ kcal/mol (0 K data). The relative stabilities do not differ largely compared to the neutral isomers, suggesting similar proton affinities of these compounds. An exception is diacetyl **12** which is considerably less stable in the protonated form, i.e., $E_{rel}(\mathbf{12}) = 7.1$ kcal/mol vs. $E_{rel}([\mathbf{12} + H]^+) = 15.8$ kcal/mol. Therefore and because loss of CO is absent for the atmospheric ion, also **12** was not included in the next stage. We note in passing that these results agree reasonably well with the literature data available: PA(**5**) = 196.9 kcal/mol, PA(**8**) = 195.2 kcal/mol, PA(**12**) = 191.7 kcal/mol, and PA(**16**) = 197.4 kcal/mol [11].

4.3. Low-energy CID

Although the CA experiments allow for a qualitative distinction of the different $C_4H_7O_2^+$ isomers, a quantitative analysis of the CID spectrum in Fig. 1 is impossible. Thus, low- and high-energy collision experiments may involve different excitation and fragmentation mechanisms and also collection efficiencies might differ for instrumental reasons [29].

An approach towards a more quantitative analysis therefore requires an examination of the dissociation behavior of $m/z = 87$ ions at low collision energies. In order to somewhat mimic the conditions in the field study, ESI was used in which the ions of interest are generated from aqueous solutions at atmospheric pressure and then extracted into a multipole detection system for CID experiments. Because memory effects in the ESI inlet system require careful cleaning between the samples (at least 1 day), we had to limit ourselves to the few isomers deduced above, namely: **5**, **7**, **8**, and **16**.

Qualitatively, the low-energy CID spectra of the corresponding protonated species (Table 3) are fully consistent with the high-energy collision experiments in the sector instrument. Thus, loss of water ($\Delta m = 18$) prevails for $[\mathbf{5} + H]^+$, eliminations of C_3H_6 ($\Delta m = 42$) and CO_2 ($\Delta m = 44$) dominate for $[\mathbf{7} + H]^+$, protonated methacrylic acid $[\mathbf{8} + H]^+$ shows a characteristic loss of CO ($\Delta m = 28$),[3] and the protonated ester $[\mathbf{16} + H]^+$ leads to the almost exclusive expulsion of methanol ($\Delta m = 32$). It is noteworthy that crotonic and vinylacetic acid do not interconvert into each other under ESI conditions as demonstrated by the fact that the respective CID spectra can clearly be distinguished. In fact, isomer differentiation is even more clean in low-energy CID than in sector MS in this particular case. Of course, the fragment abundances in low-energy CID very much depend on the actual collision energies. In this respect, the ratio of $\Delta m = 42$ and 44 is particularly instructive. At low collision energies, $\Delta m = 44$ (assigned to loss of CO_2) is favored, whereas $\Delta m = 42$ (assigned to loss of C_3H_6) gains in abundance with increasing collision energy. This energy behavior is nicely consistent with the involvement of ion/dipole complexes as suggested in Scheme 3b. At low collision energies, the collisionally excited molecules are long-lived, thereby leading to the more stable $C_3H_7^+ + CO_2$ products. At elevated collision energies, shorter complex lifetimes favor rapid dissociation and hence generation of $HOCO^+ + C_3H_6$. Finally, it is important to note for the next stage that the $C_3H_5^+$ fragment ($\Delta m = 46$) only appears at elevated collision energies.

[3] The lower intensity of CO loss in the CA spectra of the sector-field experiment compared to the low-energy CID spectra can be traced back to a discrimination of this pathway in the sector MS due to the significant KER [29].

4.4. Quantitative assay

The CID spectrum shown in Fig. 1 has been recorded with an airborne IT-MS operating at a vaguely defined collision-energy in the multicollisional regime. These conditions are required to achieve a reasonable sensitivity for the analysis of OVOCs present as trace components in the atmosphere. Nevertheless, the absence of $\Delta m = 46$, viz. $C_3H_5^+$, in Fig. 1 implies that the effective collision energy was not excessively high (see Table 3). In a pragmatic approach, let us therefore simply use the CID spectra of $[\mathbf{5} + H]^+$, $[\mathbf{7} + H]^+$, $[\mathbf{8} + H]^+$, and $[\mathbf{16} + H]^+$ recorded at $E_{lab} = 5\,eV$ with the ESI instrument for comparison. The data can be used to model the product pattern in Fig. 1 by an appropriate superposition of the relevant components (Table 4). This analysis suggests that an approximate 3:4:3 mixture of $[\mathbf{5} + H]^+$, $[\mathbf{7} + H]^+$, and $[\mathbf{16} + H]^+$ can account for the CID pattern of the atmospheric ion; a contribution of $[\mathbf{8} + H]^+$ is not indicated because no significant loss of CO is observed in the field study. It is important to point out that this approach is based on two key assumptions, namely: (i) equal sampling of the different isomers from solution in the ESI process and (ii) similar cross sections in CID at a collision energy of 5 eV.

In order to test these assumptions, a freshly prepared 3:4:3 mixture of **5**, **7**, and **16** in pure water was ionized by electrospray, the $m/z = 87$ ion mass

Table 3
Fragments[a,b] (given as mass differences Δm) in the low-energy CID mass spectra (multipole instrument) of mass-selected $C_4H_7O_2^+$ ions generated by ESI of the neutrals **5**, **7**, **8**, and **16** dissolved in pure water at various collision energies (E_{lab} in eV; collision gas: argon)[c]

	E_{lab}	18	28	32	42	44	46
[**5** + H]$^+$	5	100	5		40	30	
	10	100	2		20	7	2
	20	100			15	4	25
[**7** + H]$^+$	5	15			70	100	
	10	7	5		100	45	
	20	8	2		100	35	10
[**8** + H]$^+$	5	10	100		7	6	
	10	25	100		50	10	7
	20	40	95		100	12	60
[**16** + H]$^+$	5		3	100			
	10		4	100			
	20	1	5	100			1

[a] Normalized to the base peak (=100).
[b] Intensities derived from peak heights.
[c] Conversion to the center-of-mass frame: $E_{CM} = 0.315 \times E_{lab}$.

selected, and subjected to CID at $E_{lab} = 5$ eV. The CID spectrum of the real mixture (Fig. 2) is indeed similar to the hypothetical one as well as that of the atmospheric ion (Table 4). Of course, the agreement is by no means perfect, and more detailed analysis implies an overestimation of **16** (or a discrimination of **5** and **7**) either due to ion generation in the ESI process and/or different cross sections in CID. Some overestimation of the more volatile ester in its mixture with the related acids is in fact expected based on the recent discussion of the ESI mechanisms by Cech and Enke [30]. With regard to the noise level of Fig. 1,

Table 4
Fragments[a,b] (given as mass differences Δm) in the low-energy CID mass spectra (multipole instrument) of mass-selected $C_4H_7O_2^+$ ions generated by ESI of the neutrals **5**, **7**, **8**, and **16** dissolved in pure water, their arithmetic superposition,[c] the spectrum of a real mixture of the three leading components in pure water,[d,e] and the data for the atmospheric ion[f]

	18	28	32	42	44	46
5	56	3		22	17	2
7	8			37	55	
8	4	91		3	2	
16		3	97			
Superposition[c]	18	2	28	22	29	1
Real mixture[d,e]	18	2	41	17	22	1
Atmospheric ion[f]	17	<3[g]	28	23	26	<3[g]

[a] Normalized to $\Sigma = 100$ for all fragments.
[b] In order to improve accuracy, the CID spectra at $E_{lab} = 5$ eV were accumulated for 10–30 min, integrated peak areas, rather than heights, were considered, and several independent experiments were averaged. For these reasons, numerical differences may arise in comparison to Table 3.
[c] Optimized molar fractions of **5**, **7**, **8**, and **16**: 0.27:0.38:0:0.35.
[d] The real mixture was made using a syringe by addition of 3 μl of **5**, 4 μl of **7**, and 3 μl of **16** to 10 ml water; a contribution of **8** is not indicated. The data is the average of two independently prepared mixtures.
[e] Comparison of the superposition with the experimental data implies that **16** is overestimated by a factor of about two relative to **5** and **7** in the ESI experiments.
[f] Data derived from the raw data used for Fig. 1.
[g] Estimated from the noise level.

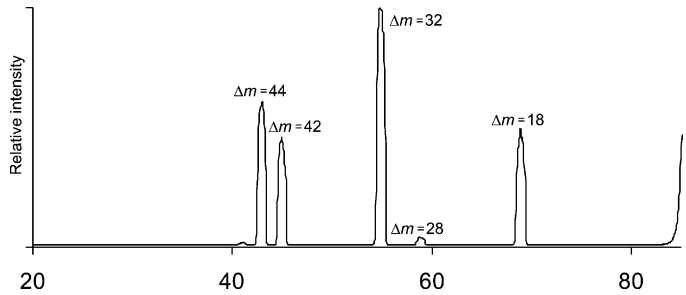

Fig. 2. Representative CID spectrum (E_{lab} = 5 eV; collision gas: argon) of the m/z = 87 ion formed by ESI of a 3:4:3 mixture of compounds **5**, **7**, and **16** in pure water.

however, any attempts to refine the analysis by explicit consideration of these effects appear supererogatory.

5. Future experiments

At first, it is to be stressed that the above analysis only allows for negative distinctions. For example, the involvement of methacrylic acid can be ruled out because no significant loss of CO is observed for the atmospheric m/z = 87 ion. Based on the CA experiments, however, a compound such as **15** could easily be admixed as a forth component at variable expenses of the others, **7** in particular. Similar considerations apply for the lactones **10** and **11** of which considerable fractions might be tolerated before conflicting with the absence of CO loss within the signal-to-noise ratio of Fig. 1. While examination of the energy-dependent CID patterns might generally help to resolve matters, it appears less helpful in this particular case because the low abundance of the atmospheric species as well as time constraints in the field studies very much limit the types of experiments which can be performed. Therefore, some complementary information must be gained. In a laboratory study, an obvious choice is the application of isotopic labeling techniques because these would allow for additional insight with minor perturbations of the systems. Quite obviously, however, there is no way to apply this approach to atmospheric trace components. Likewise, other more sophisticated methods to differentiate isomeric ions (e.g., ion/molecule reactions) are unlikely to succeed because of sensitivity limits in the atmospheric field studies. Moreover, we re-iterate the possibility outlined in the introduction that in the atmospheric field studies a "hydrated" compound Y may lead to the m/z = 87 signal investigated here.

Further, the signal for Δm = 32 observed in Fig. 1 might also be attributed to a loss of molecular oxygen, rather than methanol. Returning to the above as unlikely, but not entirely impossible considered composition $C_3H_3O_3^+$, one might anticipate the dissociation of a $C_3H_3O^+ \cdot O_2$ complex being formed in ion/molecule reactions within the ion trap in that ubiquitous $C_3H_3O^+$ ions (m/z = 55) may undergo clustering in the huge excess of oxygen compared to the trace components present in the atmosphere. While such a scenario could also be modeled in the laboratory, an ultimate conclusion is unlikely to be achieved simply because the methods available to characterize the atmospheric ion are limited. Another ambiguity with respect to the Δm = 32 fragment is associated with the m/z = 37 ion observed in Fig. 1 which is ascribed to the proton-bound dimer $(H_2O)(H_3O)^+$ formed via endothermic proton transfer of energized $C_4H_7O_2^+$ with water present in the machine followed by clustering. Association with further water molecules could lead to $(H_2O)_2(H_3O)^+$ with m/z = 55, thereby isobaric with Δm = 32 from m/z = 87. While a number of CID experiments performed with other ions in the field study [6] give no indication for the formation of water clusters larger than $(H_2O)(H_3O)^+$, this potential interference also needs to be reconsidered carefully.

Accordingly, further strategies must explore complementary means for the characterization of neutral $C_4H_6O_2$ compounds present as trace components in the terrestrial atmosphere. As far as mass spectrometry is concerned, an obvious choice is to switch from positive to negative ions because at least the free acids **5** and **7** should lead to the corresponding carboxylates with $m/z = 85$ (or their clusters), whereas the other conceivable isomers are expected to form different anions, e.g., acetate ($m/z = 59$) from **15** and acrylate ($m/z = 71$) from **16**. Likewise, detailed investigations of Spanel and Smith [7,8] suggest that also other positive ions, e.g., NO^+ or $O_2{}^+$, may be used for the identification of trace components in atmospheric gases using variants of PT-MS. Given the manifold of conceivable $C_4H_6O_2$ isomers, further laboratory studies should therefore await the results of the corresponding field studies.

6. Conclusions

The present study demonstrates that collision experiments can be used to differentiate several $C_4H_7O_2{}^+$ isomers in the gas phase [18–20]. Further, it provides a comparison of low- and high-energy collision experiments where the former allow for quantitative analysis, the latter for more rapid, qualitative insight. As far as the $m/z = 87$ ion observed in the atmospheric studies is concerned, the following conclusions can be drawn. (i) The experimentally observed $^{13}C/^{12}C$ ratio implies the composition $C_4H_7O_2{}^+$ with some contribution of carbon-depleted ions, e.g., $C_3H_3O_3{}^+$ [6]. With regard to the large excess of oxygen in the terrestrial atmosphere, particularly the formation of unusual peroxides giving rise to $C_3H_3O_3{}^+$ ions is to be considered, because these could also account for the $\Delta m = 32$ fragment. (ii) The observed CID pattern can be explained by invoking a mixture of crotonic acids (**5**, **6**), vinylacetic acid (**7**), and methyl acrylate (**16**) present as neutrals in the atmosphere. (iii) Due to sensitivity limits in the field studies, a more definitive assignment of the neutral species X giving rise to the $m/z = 87$ ion upon protonation requires the application of complementary methods to probe trace components in the terrestrial atmosphere. Mass spectrometric investigation of negative ions appear particularly promising in this respect.

Finally, let us briefly comment on the putative presence of methyl acrylate **16** in the earth's atmosphere. While carboxylic acids such as **5**–**8** may evolve from oxidative (photo-)degradations of organic compounds, the formation of the unsaturated ester **16** in atmospheric or biogenic processes appears somewhat surprising. A mere artifact from the inlet system of the airborne sampling device can be ruled out because the $m/z = 87$ ion shows a characteristic tropopause behavior at an altitude of about 10 km [6]. Instead, methyl acrylate may arise from the degradation of endogenous polymers. However, the most commonly used polyacrylates are derived from methyl methacrylate rather than **16**, such that alternative sources of methyl acrylate—or, more generally, other sources of the observed signal at $\Delta m = 32$—are to be considered as well.

Acknowledgements

This work was supported by the Deutsche Forschungsgemeinschaft, the Fonds der Chemischen Industrie, the Gesellschaft von Freunden der Technischen Universität Berlin, and the Max-Planck Gesellschaft. Further, we thank the Aventis Corporation for the generous gift of the ESI instrument and the SFB 546 for assistance in the subsidiary ESI equipment. M.S. acknowledges the Ernst Schering Research Foundation for a research fellowship.

References

[1] T. Reiner, O. Möhler, F. Arnold, J. Geophys. Res. 103 (1998) 31309.
[2] T. Reiner, O. Möhler, F. Arnold, J. Geophys. Res. 104 (1999) 13943.
[3] F. Arnold, V. Bürger, B. Droste-Fanke, F. Grimm, A. Krieger, J. Schneider, T. Stilp, Geophys. Res. Lett. 24 (1997) 3017.
[4] K. Levsen, H. Schwarz, Mass Spectrom. Rev. 2 (1983) 77.
[5] K.L. Busch, G.L. Glish, S.A. McLuckey, Mass Spectrometry/Mass Spectrometry: Techniques and Applications of Tandem Mass Spectrometry, VCH Publishers, Weinheim, 1988.

[6] A. Kiendler, F. Arnold, Int. J. Mass Spectrom. 223/224 (2003) 733.
[7] P. Spanel, D. Smith, Int. J. Mass Spectrom. Ion Processes 167/168 (1997) 375.
[8] P. Spanel, D. Smith, Int. J. Mass Spectrom. 172 (1998) 137.
[9] A. Hansel, W. Singer, A. Wisthaler, M. Schwarzmann, W. Lindinger, Int. J. Mass Spectrom. Ion Processes 167/168 (1997) 697 (and references therein).
[10] P. Spanel, D. Smith, Int. J. Mass Spectrom. 185/186/187 (1999) 139 (and references therein).
[11] E.P.L. Hunter, S.G. Lias, J. Phys. Ref. Data 27 (1998) 413.
[12] C.A. Schalley, D. Schröder, H. Schwarz, Int. J. Mass Spectrom. Ion Processes 153 (1996) 173.
[13] D. Schröder, T. Weiske, H. Schwarz, Int. J. Mass Spectrom. 219 (2002) 729.
[14] A.D. Becke, J. Chem. Phys. 98 (1993) 1372, 5648.
[15] C. Lee, W. Yang, R.G. Parr, Phys. Rev. B 37 (1988) 785.
[16] M.J. Frisch, G.W. Trucks, H.B. Schlegel, G.E. Scuseria, M.A. Robb, J.R. Cheeseman, V.G. Zakrzewski, J.A. Montgomery Jr., R.E. Stratmann, J.C. Burant, S. Dapprich, J.M. Millam, A.D. Daniels, K.N. Kudin, M.C. Strain, O. Farkas, J. Tomasi, V. Barone, M. Cossi, R. Cammi, B. Mennucci, C. Pomelli, C. Adamo, S. Clifford, J. Ochterski, G.A. Petersson, P.Y. Ayala, Q. Cui, K. Morokuma, D.K. Malick, A.D. Rabuck, K. Raghavachari, J.B. Foresman, J. Cioslowski, J.V. Ortiz, A.G. Baboul, B.B. Stefanov, G. Liu, A. Liashenko, P. Piskorz, I. Komaromi, R. Gomperts, R.L. Martin, D.J. Fox, T. Keith, M.A. Al-Laham, C.Y. Peng, A. Nanayakkara, C. Gonzalez, M. Challacombe, P.M.W. Gill, B. Johnson, W. Chen, M.W. Wong, J.L. Andres, C. Gonzalez, M. Head-Gordon, E.S. Replogle, J.A. Pople, Gaussian 98, Revision A.7, Gaussian, Inc., Pittsburgh, PA, 1998.
[17] Calculated with the Sheffield Chemputer, available: http://www.shef.ac.uk/chemistry/chemputer/index.html.
[18] H. Schwarz, T. Weiske, K. Levsen, A. Maquestiau, R. Flammang, Int. J. Mass Spectrom. Ion Phys. 45 (1982) 367.
[19] T. Weiske, H. Schwarz, Chem. Ber. 116 (1983) 323.
[20] T. Weiske, Dissertation, Technische Universität Berlin, D83, 1985.
[21] J. Loos, D. Schröder, W. Zummack, H. Schwarz, R. Thissen, O. Dutuit, Int. J. Mass Spectrom. 214 (2002) 105.
[22] C.J. Chalk, L. Radom, J. Am. Chem. Soc. 120 (1998) 8430 (and references cited therein).
[23] S.G. Lias, J.E. Bartmess, J.F. Liebman, J.L. Holmes, R.D. Levin, W.G. Mallard, J. Phys. Chem. Ref. Data 17 (1988) Suppl. 1.
[24] NIST Chemistry WebBook, NIST Standard Reference Database Number 69, in: P.J. Linstrom, W.G. Mallard (Eds.), National Institute of Standards and Technology, Gaithersburg, MD, July 2001, 20899 (http://webbook.nist.gov).
[25] W. Koch, M.C. Holthausen, A Chemist's Guide to Density Functional Theory, Wiley-VCH, New York, 2000.
[26] J. Cioslowski, M. Schimeczk, G. Liu, V. Stoyanov, J. Chem. Phys. 113 (2000) 9377.
[27] J. Cioslowski (Ed.), Quantum-Mechanical Prediction of Thermochemical Data, Kluwer, Dordrecht, 2001.
[28] M. Semialjac, J. Loos, D. Schröder, H. Schwarz, Int. J. Mass Spectrom. 214 (2002) 129.
[29] B.A. Rumpf, C.E. Allison, P.J. Derrick, Org. Mass. Spectrom. 21 (1986) 295.
[30] N.B. Cech, C.G. Enke, Mass Spectrom. Rev. 20 (2001) 362.